http://dx.doi.org/10.5012/bkcs.2013.34.2.510

Hot-Pressing Effects on Polymer Electrolyte Membrane Investigated by ^{2}H NMR Spectroscopy

Sang Man Lee[a] and Oc Hee Han[†,‡,*]

Daegu Center, Korea Basic Science Institute, Daegu 702-701, Korea. [*]E-mail: ohhan@kbsi.re.kr
[†]Graduate School of Analytical Science & Technology, Chungnam National University, Daejeon 305-764, Korea
[‡]Department of Chemistry, Kyungpook National University, Daegu 702-701, Korea
Received December 22, 2012, Accepted December 27, 2012

The structural change of Nafion polymer electrolyte membrane (PEM) induced by hot-pressing, which is one of the representative procedures for preparing membrane-electrode-assembly for low temperature fuel cells, was investigated by ^{2}H nuclear magnetic resonance (NMR) spectroscopy. The hydrophilic channels were asymmetrically flattened and more aligned in the membrane plane than along the hot-pressing direction. The average O-^{2}H director of ^2H_2O in polymer electrolyte membrane was employed to extract the structural information from the ^{2}H NMR peak splitting data. The dependence of ^{2}H NMR data on water contents was systematically analyzed for the first time. The approach presented here can be used to understand the chemicals' behavior in nano-spaces, especially those reshaping and functioning interactively with the chemicals in the wet and/or mixed state.

Key Words : NMR spectroscopy, Membrane, Hot-pressing, Nafion, Hydrophilic channel

Introduction

Proton conductivity in polymer electrolyte membrane (PEM) fuel cells strongly depends on PEM hydrophilic channel structure[1-6] as well as the content and distribution of water within the PEM.[4-10] Shortening proton-conduction pathway lengths by aligning more hydrophilic channels perpendicular to the PEM plane would be desirable to enhance proton conductivity.[3] The structure and alignment of PEM hydrophilic channels tends to be strongly influenced by membrane-electrode-assembly (MEA) preparation methods such as hot-pressing,[8,11-14] polymer processing for membrane production,[5,6,13-15] and swelling degree.[4-6,15-17] Thus, it is desirable to study the PEM in wet states in order to probe the proton conduction within and the hydrophilic channel structures of the functioning PEM. PEM hydrophilic channels have been primarily investigated by scattering techniques using neutrons and X-rays,[3-5,12-14,16-18] however, these techniques detect both systematic ordering of the hydrophobic polymer backbone and hydrophilic clusters. In contrast, various nuclear magnetic resonance (NMR) methods have been used to probe water dynamics in the hydrophilic clusters as well as the cluster structures. For example, pulsed field gradient (PFG) methods have been used to detect self diffusions of water and to correlate them with proton conductivities.[3,12,15,19,20] Field-cycling NMR relaxometry was used to detect water dynamics in ionomer membranes.[21] Peak splitting data of ^{2}H NMR spectra[3,15,19,20,22-29] have been used to investigate hydrophilic channel alignments, and they naturally detect the influence of water used as a probing molecule. Although similar information can be obtained with ^{1}H NMR spectra,[30] ^{2}H NMR spectra are better since they do not have background signals. ^{2}H NMR studies on Nafion swelled in ^2H_2O have revealed that the hydrophilic channel ordering occurs along the stretching direction[3] and that the ordering difference occurs according to polymer processing methods.[15] Peak splitting of ^{2}H NMR spectra has been used to measure the parameters that are related to the order of the molecules or molecular segments to the reference axis.[27,28] The ordering results from the inherent nature of molecules and/or their anisotropic environments. The anisotropic matrix forces probing molecules to move anisotropically and/or stay in a certain direction for a relatively longer period of time. In turn, this anisotropic dynamics generate partial ordering of the probe molecules. Thus, to date, peak splitting of ^{2}H NMR spectra has been widely used to determine the anisotropic dynamics of probe molecules and/or anisotropic structures of the matrix.[3,15,19,20,22-29]

In this work, the average O-^{2}H director of ^2H_2O in PEM was employed to extract the structural information from ^{2}H NMR data and applied to detect the structural change of Nafion induced by hot-pressing, which is one of the representative procedures for preparing MEAs for low temperature fuel cells. For the first time, the dependence of ^{2}H NMR data on the water content in PEM was systematically interpreted in terms of channel shape, size, and ordering. Additionally, the relationship between ^{2}H NMR data, reflecting both ^{2}H exchange and diffusion, and proton conduction through the Grotthuss[31] and vehicle mechanisms was discussed.

Experimental

No stress applied Nafion (NS) membranes were prepared

[a]Present Address: Raw Materials Research Group, Technical Research Laboratories, POSCO, Pohang 790-300, Korea

by pretreating commercially available Nafion 117 as previously reported.[11] Hot-pressed Nafion (HP) was prepared by hot-pressing NS membranes at 100 kg/cm^2 and 135 °C for 3 min. For comparison, stretched Nafion (ST) membranes were prepared by stretching of the length by 1.5× at room temperature. The samples were then trimmed to match the sample space (14.0 mm × 3.0 mm) of the rectangular sample holder consisting of two rectangular Teflon sheets (14.0 mm × 3.5 mm × 1 mm) and then swelled in ^2H_2O for at least 12 h. The free surface water was wiped out before the swelled membrane was placed in a sample holder. The holder with the sample was then wrapped in Teflon tape and inserted into a 5-mm NMR tube. For the Z axis rotation experiment, a sample size of 3 mm × 3 mm was used with an appropriate sample holder. All of the ^{2}H NMR experiments were performed at room temperature at a magnetic field of 14.1 T and a wideline probe with a horizontal solenoid coil with a 5-mm inner diameter was used. A pulse length of 6 μs, a pulse repetition delay time of 2 s, and 32 or 128 scans were used to acquire a ^{2}H spectrum. Membrane thickness in the dry state was 0.17, 0.16, and 0.14 mm for the NS, ST, and HP membranes, respectively. Masses of swelled membranes were determined gravimetrically before and after the NMR experiments to confirm a negligible variation of water content in the membrane. The water content of the swelled membrane was calculated as the mass difference between the dry and swelled membranes. The mass of the dry membrane was measured after the membrane was dried under a vacuum at room temperature until no further mass change was detected.

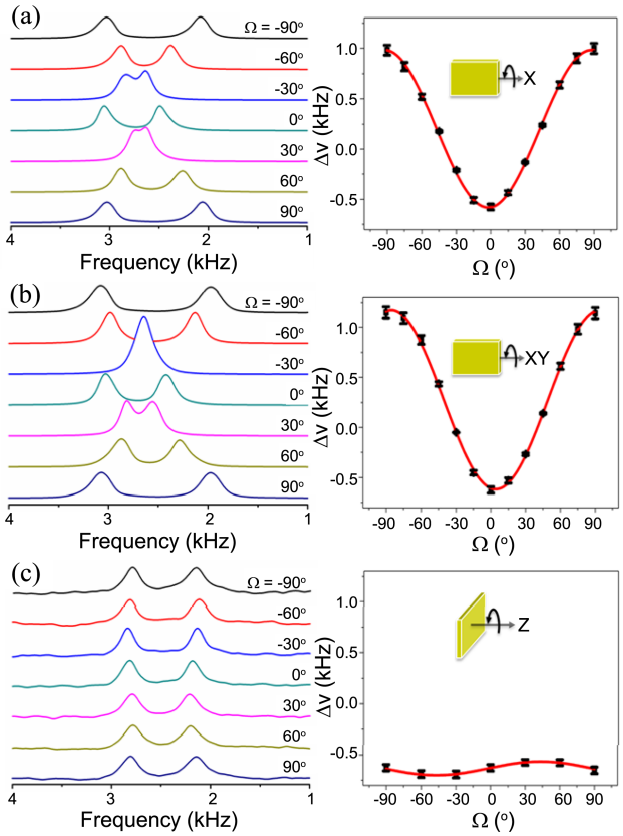

Figure 1. ^{2}H NMR spectra (left) and ^{2}H peak splittings (right) of hot-pressed Nafion versus rotation angle for the rotation axes of (a) X, (b) XY, and (c) Z. The ^2H_2O contents were 18, 19, and 15 wt % for (a), (b), and (c), respectively.

Results and Discussion

The ^{2}H spectra of the HP membranes (Figure 1(a)-1(c)) were acquired at each sample rotation angle Ω between an external magnetic field H_0 and the axis P, orthogonal to the rotation axis R, in the membrane (Figure 2(a)). The ^2H_2O contents in the membrane were similar (18, 19, and 15 wt % for Figure 1(a), 1(b), and 1(c), respectively). The axes in the membrane were defined as shown in Figure 2(b). The peak splitting pattern for the Z axis rotation was dramatically different from those for the X and XY axes rotation (Figure 1). These peak splitting patterns can be interpreted using equation (1) below, which was adapted from Eq. (3) in reference 29, where the peak splitting (Δν) is a function of the residual quadrupole coupling constant ($\Delta\nu_0$), the polar angle (θ) and the azimuthal angle (φ) of the electric field gradient tensor of average O-^{2}H director in a magnetic field (H_0) (Figure 2(c)), and $\eta = (V_{xx} - V_{yy})/V_{zz}$:

$$\Delta\nu = (1/2)\Delta\nu_0(3\cos^2\theta - 1 + \eta\sin^2\theta\cos2\varphi). \quad (1)$$

For $\eta = 0$, the equation is simplified to $\Delta\nu = (1/2)\Delta\nu_0(3\cos^2\theta - 1)$. When the membrane is rotated in a magnetic field, θ and φ become functions of Ω, polar angle (α), and azimuthal angle (β) of the average O-^{2}H director in the XYZ axis system (Figure 2). Refer to the relationships among θ, Ω, α, and β described in Supporting Information for an explanation of the explicit relationships among θ, α, β, and Ω. If the average O-^{2}H director is aligned with the Z rotation axis (θ, ~90°; φ, a constant angle), the peak splitting must barely

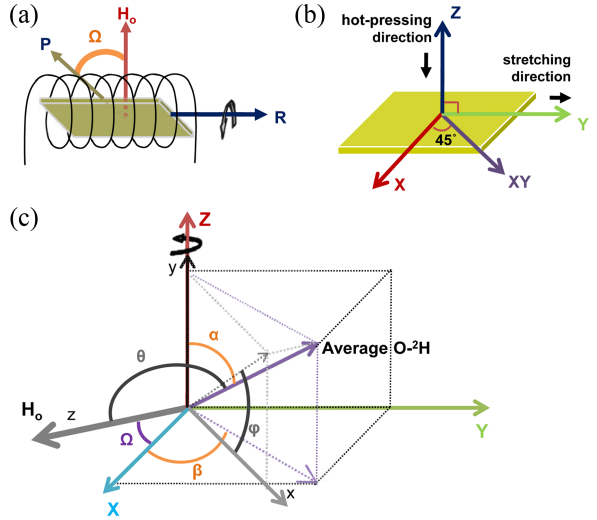

Figure 2. (a) Definition of membrane rotation angle, Ω, between the magnetic field H_0 and the P axis, in the membrane, orthogonal to the rotation axis, R. (b) Definition of the XYZ axes in the membrane. (c) Definition of the angles and axes used in equation (1) for the Z axis rotation.

change for the Z axis rotation as observed in Figure 1(c). The φ value depends on the definition of x and y axes (the magnetic field axis system relative to the average O-^{2}H director), in our case, the y axis was aligned with the rotation axis (Figure 2(c)). In contrast, for rotation around the X or XY axes, both the absolute magnitude of the peak splitting and its sign varied when Ω changed. This finding indicates that the average O-^{2}H director of ^2H_2O in the HP samples crosses the magic angle (54.7°) versus H_0 during the membrane rotations. This means the director was aligned with neither the X nor the XY axes and that it deviated more than 54.7° from these axes. This finding was in agreement with the prediction of the average O-^{2}H director, which was closely aligned with the Z axis. The data fitting of Δν values measured from the spectra to Eq. (1) by adjustment of the $\Delta\nu_0$, η, α, and β values is shown in the plots of Figure 1(a)-1(c). η was nearly 0 and the orientation of the average O-^{2}H director, with the α (15 ± 0.5°) and β (47 ± 2°) values that generated from the fitting, is schematically shown in Figure 3. As predicted qualitatively, the angle between the average O-^{2}H director and the Z axis, 15 ± 0.5°, was much smaller than 54.7°.

ST membranes have been extensively studied using various techniques, and the results have indicated that hydrophilic channels and/or polymer chains were induced to improve alignment along the stretching direction.[3,18,20,25-29] The average direction of the hydrophilic channels was interpreted to coincide with the average O-^{2}H director.[3,15,20] Our ^{2}H NMR results of minimally changing peak splitting for the Y axis rotation (Figure S1 in Supporting Information) also indicate that the average O-^{2}H director is closely aligned with the stretching direction (Y axis) being identical with the average hydrophilic channel direction. The average O-^{2}H director can be considered as the vector sum of all of the factors influencing the director, *i.e.*, the interaction of water with the inner surface of the hydrophilic channels, deuteron exchange and diffusion, and water mobility in the channels, *etc*. This interpretation is possible since only the vector components parallel to the channel directions remain if the vector components in the cross-section planes of the hydrophilic channels are cancelled out. Consequently, if the channel cross-section is sufficiently symmetrical to cancel out the vector components in the cross-section planes, the average O-^{2}H director will coincide with the average channel direction as seen in the ST membranes. On the other hand, if the channel cross-sections are not sufficiently symmetrical, there will be residual components of the individual O-^{2}H directors in the cross-sectional planes and the average O-^{2}H director orientation will deviate from the channel direction. Thus, the fact that the average O-^{2}H director was oriented close to the Z rotation axis indicates that either the cross-sections of the hydrophilic channels in the HP membranes were far from symmetrical or the channels themselves were, on average, aligned in the through-plane direction. According to earlier reports using scattering techniques and conductivity measurements, hot-pressing induced lamellar alignment of polymers and/or hydrophilic channels in the in-plane

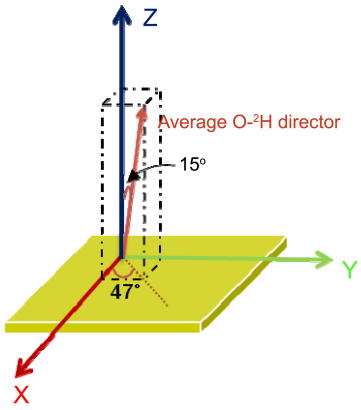

Figure 3. Orientation of the average O-^{2}H director of ^2H_2O in the hot-pressed Nafion membrane obtained from the fitting of ^{2}H peak splitting values using the equation described in the text.

directions and increased in-plane conductivity.[13,14] Thus, our ^{2}H NMR results together with the scattering and conductivity data indicate that the hydrophilic channels were rather asymmetrically flattened in a manner perpendicular to the compressed direction.

The similar spectral patterns of the HP membranes for the X and XY rotations indicate that the channels are either overall randomly oriented in all directions or circularly oriented in the membrane plane. However, the channels would rarely be in circular alignment unless they were so prior to the hot-pressing. In general, prior to post-processing the channels were known to form randomly oriented bundles rather than to circularly align.[4,18] The hot-pressing process compressed the membranes in the Z direction and simultaneously expanded them about 30 ± 10% in each in-plane direction. This expansion indicates that the channels were forced to further align in each in-plane direction as predicted by the ST membrane results.[3,18,20] The peak splitting of each NS membrane was observed for the purpose of comparison with the starting materials. However, the peak splitting of each NS membrane saturated with ^2H_2O (Figure S2(a) and S2(b) in Supporting Information) was too small for determination of the average channel orientation. The ^2H_2O contents of the NS membranes were reduced for larger peak splitting (Figure S2(c) in Supporting Information). However, the resulting peak splitting was still not large enough to enable patterns of the 3 different rotation axes to be distinguished. This finding implies that the sizes of the hydrophilic channels in the NS membranes were relatively large compared with those in the ST and HP membranes.

Strong dependence of the $\Delta\nu_0$ value on the membrane water content (Figure 4) was consistent with the results of earlier reports[15,19] that showed Δν values at a certain orientation, rather than $\Delta\nu_0$ values. Here a single $\Delta\nu_0$ value extracted from a set of Δν values does not depend on magnetic field orientation. The ^{2}H peak splitting versus temperature was reported to vary at the same ratio in all directions, suggesting change in the size but not of the shape of channels.[15] Likewise if the water content variation changes the size but not the shape of the channels and if the $\Delta\nu_0$ value is related

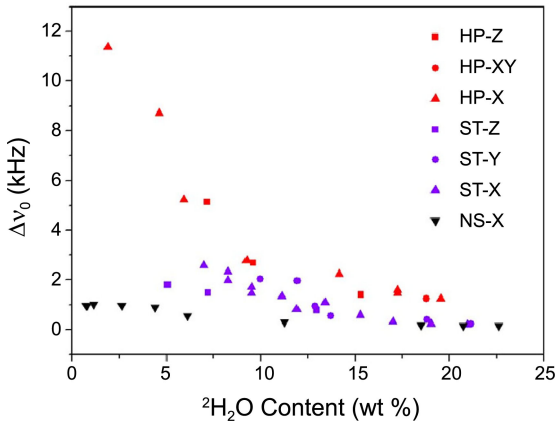

Figure 4. Residual quadrupole coupling constants ($\Delta\nu_0$) of deuterium nuclear magnetic resonance data of hot-pressed (HP), stretched (ST), and no stress applied (NS) Nafion membranes versus ^2H_2O content in the membranes. The rotation axis of the membranes in the magnetic field is designated with the membrane type notation in the inset.

with the surface-to-volume ratio of hydrophilic channels,[15,19] the $\Delta\nu_0$ value becomes proportional to the inverse of a channel radius r (refer to the explanation of the relationship between $\Delta\nu_0$ and water content in Supporting Information for the explanation in detail). Here each straight segment of channels is regarded as an individual channel so that channel tortuosity is reflected in the $\Delta\nu_0$ value. Then the proportional constant δ becomes a function of channel alignment, shape, and size relative to the anisotropic interaction length. As a result, $\Delta\nu_0 = \delta/r$ where $\delta = \delta_1\delta_2\delta_3\delta_4$; δ_1, δ_2, δ_3, and δ_4 are proportional constants related with channel alignments, channel shapes, channel size relative to the anisotropic interaction length, and the ratios of channel lengths to radii, respectively. Here diffusion path lengths can be taken as an example of anisotropic interaction lengths. When at least one of the dimensional lengths of the channel becomes smaller than the diffusion path lengths as a result of the water content reduction, diffusion in that direction changes to a restricted one; consequently, δ_3 changes to a bigger constant. Among δ_n (n = 1, 2, 3, and 4), only δ_3 can be a function of water content. When δ is not a function of water content, the plots of $\Delta\nu_0$ versus water content for different δ values would result in the same curve shapes with different slopes. Figure 4 also shows different $\Delta\nu_0$ values for membranes with the same water content, but prepared by different post-processing methods. The water content in wt % is proportional to the volume of water and, in turn, to the channel volume filled with water in the membrane. Thus if the channel shape, size, and alignment were not changed by post-processing, the $\Delta\nu_0$ value should be the same at the same water content. However, the largest $\Delta\nu_0$ values for the HP membranes and the smallest $\Delta\nu_0$ values for the NS membranes were observed at the same water content. Therefore, membrane post-processing, such as hot-pressing and stretching, induced the changes of channel shape, size, and/or alignment. These changes were not relaxed even after several months.[32] A more drastic change of HP membrane data than other membrane data versus water content in Figure 4 implies the change of the proportional constant for the water content variation (*i.e.*, change of δ_3). This indicates that at least one of the channel dimensions of HP membranes is much shorter than those of other membranes at the same water content. This can mean that the channel diameters were reduced and/or that the channels were flattened by hot-pressing. ST membranes were found to have the channel domains aligned along the stretching direction without elongation of channels.[3,19] This result suggests that the flattened channels are possible without the elongation of channel lengths or the reduction of channel cross-section areas. This interpretation is also consistent with the channels flattened by hot-pressing found during the investigation of the channel shapes and alignments described previously in this article.

Proton transport in water was known to occur more effectively through the Grotthuss mechanism than through the vehicle mechanism.[31] In the Grotthuss mechanism, proton charges travel through water network by rapid (< 100 fs) interchange of hydrogen bonding and covalent bonding without physical proton transport.[31] Therefore, ^1H spins observed using NMR must be average forms of protons and hydrogens in water molecules. Deuteron exchange due to the Grotthuss mechanism occurs in a much shorter time frame than NMR signal acquisition, even when influence of heavier deuteron than proton on the exchange reaction is considered. This deuteron exchange as well as ^2H diffusion is reflected in ^2H peak-splitting data. A single pair of peaks resulting in a single peak splitting for each spectrum indicates that the structures ^2H_2O probed were interconnected enough for ^2H_2O to sense all of the structures and exchange deuterons in the NMR time scale. Consequently, average structural information was obtained from the ^2H NMR data. If the ^2H_2O in each domain cannot sense other domains with the different structure and orientation versus H_0 or in different ^2H_2O content, many pairs of ^2H_2O peaks can appear in a spectrum.[15] Therefore, we allowed enough time for ^2H_2O to spread and reach equilibrium in the membrane before conducting the NMR experiments.

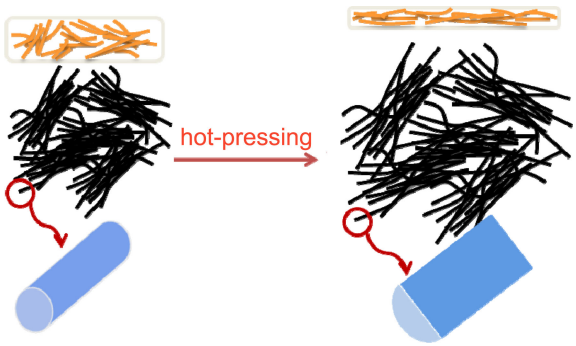

Figure 5. Schematics of hydrophilic channels in hot-pressed and no stress applied Nafion. The black color shows the top view of hydrophilic channels in the membrane, the orange color shows the side view, and the blue color shows the shape of the cross-section of a single channel. The asymmetric cross-section for the hot-pressed membrane is represented as a half-circle which is just one of many possible asymmetric shapes.

Conclusion

Hydrophilic channels of HP were flattened asymmetrically and more aligned in the membrane plane than along the hot-pressing direction. However, the orientation of the channels in the plane was random as schematically shown in Figure 5. The average O-^{2}H director of ^2H_2O in the Nafion membranes was used to interpret the ^{2}H NMR data and the orientation of the director was recognized with a nearly constant peak splitting for the sample rotation in a magnetic field. The dependence of peak splitting on water content was systematically correlated with channel alignments, shapes, and sizes relative to anisotropic interaction lengths. The ^{2}H peak splitting data reflect both ^{2}H exchange and diffusion; hence, they effectively describe proton conduction by the Grotthuss and vehicle mechanisms. In addition, ^{2}H peak splitting data are sensitive to morphological and alignment difference on a nano-scale and are complementary to PFG and/or scattering data. Application of this method can be extended to probe molecules' behavior in nano-spaces, especially those reshaping and functioning interactively with the chemicals in the wet and/or mixed state.

Acknowledgments. This work was supported by the KBSI grants (K29030, K30030, and K31030) to O.H. Han and by the National Research Foundation of Korea Grant funded by the Korean Ministry of Education, Science and Technology (2012, University-Institute cooperation program). Juhee Lee at the KBSI and Ryeo Yun Hwang at GRAST CNU are acknowledged for their assistance to prepare the figures.

Supporting Information Available. The relationships among θ, Ω, α, and β were derived. Representative ^{2}H NMR spectra of the stretched Nafion 117 membranes (Figure S1) and the Nafion 117 membranes without any stress applied (Figure S2) obtained at 3 different rotation axes were shown. The relationship between $\Delta\nu_0$ and water content was derived.

References

1. Samulski, E. T. *Nature Mater.* **2011**, *10*, 486.
2. Spiess, H. W. *Macromolecules* **2010**, *43*, 5479.
3. Li, J.; Park, J. K.; Moore, R. B.; Madsen, L. A. *Nature Mater.* **2011**, *10*, 507.
4. Schmidt-Rohr, K.; Chen, Q. *Nature Mater.* **2008**, *7*, 75.
5. Mauritz, K. A.; Moore, R. B. *Chem. Rev.* **2004**, *104*, 4535.
6. Elabd, Y. A.; Hickner, M. A. *Macromolecules* **2011**, *44*, 1.
7. Kreuer, K.-D.; Paddison, S. J.; Spohr, E.; Schuster, M. *Chem. Rev.* **2004**, *104*, 4637.
8. Cappadonia, M.; Erning, J. W.; Niaki, S. M. S.; Stimming, U. *Solid State Ionics* **1995**, *77*, 65.
9. Anantaraman, A. V.; Gardner, C. L. *J. Electroanal. Chem.* **1996**, *414*, 115.
10. Pourcelly, G.; Oikonomou, A.; Gavach, C.; Hurwitz, H. D. *J. Electroanal. Chem.* **1990**, *287*, 43.
11. Jung, S. Y.; Han, O. H. *Bull. Korean Chem. Soc.* **2009**, *30*, 1559.
12. Hensley, J. E.; Way, J. D.; Dec, S. F.; Abney, K. D. *J. Membr. Sci.* **2007**, *298*, 190.
13. Park, M. J.; Balsara, N. P. *Macromolecules* **2010**, *43*, 292.
14. Ma, S.; Siroma, Z.; Tanaka, H. *J. Electrochem. Soc.* **2006**, *153*, A2274.
15. Li, J.; Wilmsmeyer, K. G.; Madsen, L. A. *Macromolecules* **2009**, *42*, 255.
16. Gierke, T. D.; Munn, G. E.; Wilson, F. C. *J. Polym. Sci.: Polym. Phys. Ed.* **1981**, *19*, 1687.
17. Young, S. K.; Trevino, S. F.; Beck Tan, N. C. *J. Polym. Sci. Part B: Polym. Phys.* **2002**, *40*, 387.
18. van der Heijden, P. C.; Rubatat, L.; Diat, O. *Macromolecules* **2004**, *37*, 5327.
19. Hou, J.; Li, J.; Madsen, L. A. *Macromolecules* **2010**, *43*, 347.
20. Park, J. K.; Li, J.; Divoux, G. M.; Madsen, L. A.; Moore, R. B. *Macromolecules* **2011**, *44*, 5701.
21. Perrin, J.-C.; Lyonnard, S.; Guillermo, A.; Levitz, P. *Magn. Reson. Imaging* **2007**, *25*, 501.
22. Rankothge, M.; Haryadi; Moran, G.; Hook, J.; Van Gorkom, L. *Solid State Ionics* **1994**, *67*, 241.
23. Chen, R. S.; Jayakody, J. P.; Greenbaum, S. G.; Pak, Y. S.; Xu, G.; McLin, M. G.; Fontanella, J. J. *J. Electrochem. Soc.* **1993**, *140*, 889.
24. Bureekaew, S.; Horike, S.; Higuchi, M.; Mizuno, M.; Kawamura, T.; Tanaka, D.; Yanai, N.; Kitagawa, S. *Nature Mater.* **2009**, *8*, 831.
25. Aguilera-Mercado, B. M.; Genesky, G. D.; Duncan, T. M.; Cohen, C.; Escobedo, F. A. *Macromolecules* **2010**, *43*, 7173.
26. Albunia, A. R.; Graf, R.; Grassi, A.; Guerra, G.; Spiess, H. W. *Macromolecules* **2009**, *42*, 4929.
27. Callaghan, P. T.; Samulski, E. T. *Macromolecules* **2003**, *36*, 724.
28. Deloche, B.; Samulski, E. T. *Macromolecules* **1981**, *14*, 575.
29. Matsumura, K.; Hayamizu, K.; Yamamoto, O. *J. Polym. Sci. Part B: Polym. Phys.* **1989**, *27*, 2407.
30. Prestegard, J. H.; Al-Hashimi, H. M.; Tolman, J. R. *Q. Rev. Biophys.* **2000**, *33*, 371.
31. Woutersen, S.; Bakker, H. J. *Phys. Rev. Lett.* **2006**, *96*, 138305.
32. Xie, T. *Nature* **2010**, *464*, 267.